

ORIGINAL ARTICLE OPEN ACCESS

Spiroplasma Display an Intricate Continuum of Infection Heterogeneity and Persistence in *Myrmica* Ants

Diego Castillo Franco¹  | Thomas Parmentier^{1,2}  | Tessa Van de Walle¹ | Emma Van Reempts¹ | Wouter Dekoninck³ | Jonathan Romiguier⁴ | Nicky Wybouw¹ ¹Department of Biology, Ghent University, Ghent, Belgium | ²Unit of Social Ecology, Département de Biologie des Organismes, Université Libre de Bruxelles, Brussels, Belgium | ³Royal Belgian Institute of Natural Sciences, Brussels, Belgium | ⁴ISEM, University of Montpellier, CNRS, IRD, Montpellier, France**Correspondence:** Nicky Wybouw (nicky.wybouw@ugent.be)**Received:** 12 September 2025 | **Revised:** 2 March 2026 | **Accepted:** 28 March 2026**Keywords:** co-infection | endosymbiosis | maternal transmission | social insects

ABSTRACT

Many bacterial taxa evolved facultative symbiotic associations with insects and spread through host populations by horizontal and maternal transmission. Co-infection at the individual host level may facilitate or constrain the spread of facultative symbionts. Due to insufficiently detailed genotyping, co-infections of maternally transmitted symbionts often remain hidden, limiting our understanding of (co-)infection dynamics. *Spiroplasma* bacteria exhibit multiple independent origins of symbiosis with insects and have poorly understood patterns of transmission and co-infection. Here, we examined these traits of *Spiroplasma* symbiosis using *Myrmica* ants, a system known for high frequencies of single *Spiroplasma* infections. Through exhaustive genotyping of 75 colonies across seven *Myrmica* species, we uncovered multiple cryptic co-infections involving two distinct *Spiroplasma* clades that display significantly different infection frequencies in workers. Within *Myrmica ruginodis*, infection heterogeneity was contingent on ant caste and was lower in workers. Remarkably, the sMyr *Spiroplasma* variant infected four *Myrmica* species and was widespread in queens and workers. We provide phylogenomic and functional genomic support for an exceptionally stable symbiosis with maternally acquired sMyr, with a predicted infection persistence of seven million years in the *Myrmica scabrinodis* species group. Our findings reveal that *Spiroplasma* can display complex infection heterogeneity and evolve an evolutionary stable maternally acquired infection within insect hosts.

1 | Introduction

Heritable bacterial symbionts form an important component of the ecology and evolution of their animal host, including many insects. In insects, symbioses can be differentiated by whether the heritable bacterial infection is essential for the survival and reproduction of the host. Many plant- and blood-feeding insect taxa rely on obligate bacterial symbionts to survive on an unbalanced supply of dietary nutrients. These nutritional symbioses are typified by co-cladogenesis whereby the host and symbiont co-diversify into a contemporary set of genetically divergent lineages or species

(García-Lozano et al. 2024; Hosokawa et al. 2006, 2012). Although not a universal feature, these obligate symbioses can persist for 10s of millions of years by cladogenic acquisition (García-Lozano et al. 2024; McCutcheon et al. 2019; McCutcheon and Moran 2010; Tamas et al. 2002). In contrast, maternally inherited facultative symbionts are not essential for their insect hosts. Although facultative maternally transmitted symbionts can reach near-fixation frequencies in host populations, these infections are considered to be lost on shorter timescales than insect speciation. Here, infection loss is balanced by horizontal transmission into related and distant host lineages (Sanaei et al. 2021). Maternal transmission efficiency

Diego Castillo Franco and Thomas Parmentier contributed equally to this study.

This is an open access article under the terms of the [Creative Commons Attribution-NonCommercial](https://creativecommons.org/licenses/by-nc/4.0/) License, which permits use, distribution and reproduction in any medium, provided the original work is properly cited and is not used for commercial purposes.

© 2026 The Author(s). *Molecular Ecology* published by John Wiley & Sons Ltd.

and subsequent proliferation in developing offspring tissues are also key determinants of how facultative symbionts spread and persist in host populations. Maternal transmission is often imperfect in natural insect populations, predicted to decrease the prevalence of infected hosts and infection persistence (Brenninger et al. 2025; Hague et al. 2020; Hamm et al. 2014; Hoffmann et al. 1990).

To spread through insect populations, maternally transmitted facultative symbionts induce a variety of reproductive phenotypes, including cytoplasmic incompatibility (CI) and male killing (MK). CI causes embryonic mortality when infected males fertilize uninfected females. Embryonic survival is rescued when females are infected, promoting the spread of maternally transmitted symbionts. MK promotes the fitness of infected females in multiple ways, including by reduced levels of competition and inbreeding (Engelstädter and Hurst 2009). CI and MK are associated with multiple symbiotic bacteria, including *Rickettsia*, *Wolbachia* and *Spiroplasma* (Engelstädter and Hurst 2009; Harumoto and Lemaitre 2018; Hurst et al. 2000; Owashi et al. 2024; Pollmann et al. 2022; Shropshire et al. 2020). For sMel *Spiroplasma*, the *spaid* gene controls MK (Harumoto and Lemaitre 2018). *Spaid* carries ankyrin repeats and a deubiquitinase domain that disrupt the genome-wide transcription and segregation behaviour of the male X chromosome (Cheng et al. 2016; Harumoto et al. 2016; Harumoto and Lemaitre 2018). For *Wolbachia*, *cif* genes underpin CI and encode for CifA and CifB effectors. To induce CI, CifB effectors are essential in infected males. CifA effectors may also contribute to CI induction, but are universally essential for CI rescue in infected females (Beckmann et al. 2017; LePage et al. 2017). Comparative genomics uncovered that other maternally transmitted symbionts also carry *cif* genes, including *Spiroplasma* (Amoros et al. 2025). Interestingly, in 2022, CI has been reliably demonstrated for sDis *Spiroplasma*, a variant that infects the parasitoid wasp *Lariophagus distinguendus* (Pollmann et al. 2022). However, genome analysis of sDis did not reveal clear homologs to *cif* genes (Pollmann et al. 2022). Whether *cif* genes or an independent genetic basis underpin CI in *Spiroplasma* remains an open question.

Heritable facultative symbionts can also spread by increasing the relative fitness of infected individuals without necessarily altering host reproduction. An important symbiont-mediated fitness benefit is a stronger protection against parasites and pathogens (Ballinger and Perlman 2019). In insect hosts, *Spiroplasma*-induced protection against parasitic nematodes and wasps is controlled by ribosome-inactivating protein effectors (RIPs) (Ballinger and Perlman 2017, 2019). Based on genome sequencing, a previous study has also proposed a protective role of *Spiroplasma* against viral infection in a deep-sea sea cucumber host (He et al. 2018).

For some reproductive symbionts such as *Wolbachia*, surveys have shown that individual insects can carry divergent variants, here also described as infection heterogeneity (Kondo et al. 2005; Miyata et al. 2024). Empirical and theoretical work shows that infection heterogeneity at the individual level may facilitate the spread of these variants through their combined effects on host fitness and reproduction (Engelstädter et al. 2004; Frank 1998; Kondo et al. 2005; Miyata et al. 2024; Zug and Hammerstein 2018). Infection heterogeneity can, however, be constrained by microbe-microbe competition (Itoh et al. 2019; Worsley et al. 2021). Imperfect maternal transmission and subsequent proliferation can create a

complex suite of polymorphic infection states within a population or species, especially if these rates differ between the co-infecting variants. Due to a lack of sufficiently detailed genotyping, co-infections of maternally transmitted symbionts often remain hidden, especially for closely related co-infecting variants. This limits our understanding of the dynamics of infection heterogeneity of facultative symbionts and is pertinent for social insects that evolved caste determination. Some studies of social insects have indicated that infection frequencies of facultative symbionts may vary between reproductive and non-reproductive castes (Treanor et al. 2018). These infection patterns may be caused by preferential transmission of symbionts towards queens. Alternatively, transmission rates to reproductive and non-reproductive castes could be equal, but infection could be constrained in workers due to an underdevelopment of reproductive tissues (Treanor et al. 2018). How these transmission biases may impact infection heterogeneity across castes remains unresolved.

Spiroplasma are cell wall-less bacteria that belong to a broad group of host-associated Mollicutes that includes vertebrate-, plant- and invertebrate-associated symbionts. Insect-associated *Spiroplasma* variants have been placed in several phylogenetic groups, including the Citri, Poulsonii and Ixodetis clades (Ballinger and Perlman 2019). Compared to other facultative symbionts, *Spiroplasma* bacteria display a wide continuum in the frequency of horizontal versus maternal transmission. Whereas some *Spiroplasma* lineages are strictly horizontally acquired, other lineages independently evolved the ability to be maternally transmitted, creating highly variable and unpredictable patterns of infection heterogeneity and spread (Moore and Ballinger 2023). The Citri clade of *Spiroplasma* harbours a complicated mixture of variants with varying transmission strategies, raising questions on how long Citri infections might persist in an insect host (Bové et al. 2003; Clark et al. 1985; Moore and Ballinger 2023; Saillard et al. 1987).

A previous study uncovered high frequencies of single infections of Citri *Spiroplasma* in multiple *Myrmica* lineages (Ballinger et al. 2018). Using single-locus markers, a trend towards co-cladogenesis was suggested but could not be formally demonstrated due to insufficient host information and sequence data. Moreover, the timing of the putative cladogenic spread of *Spiroplasma* and the species identity of the *Myrmica* hosts remain unclear. Transcriptomic profiling of a polygynous *Myrmica ruginodis* colony suggested that two *Spiroplasma* variants may be segregating, raising the question of whether different queens carry divergent variants or whether there may be a co-infection at the individual level (Ballinger et al. 2018; Morandin et al. 2016). Although previous genome assemblies, derived from polygynous *Myrmica* field colonies, could not be attributed to single *Spiroplasma* variants, candidate RIPs were observed, indicating that at least some *Myrmica*-associated variants might mediate protection against parasites. Together, these observations identify the *Myrmica* genus as an interesting system to examine infection frequency, heterogeneity and persistence of insect-associated *Spiroplasma*. In the current study, we further dissected *Spiroplasma* symbiosis in *Myrmica* ants by leveraging Sanger, Oxford Nanopore and Illumina sequencing of eggs, workers and queens. We uncovered cryptic infection heterogeneity in multiple *Myrmica* species and unravelled how castes may shape infection heterogeneity in *Myrmica ruginodis*.

Exhaustive field sampling uncovered the presence of cryptic *Ixodetis Spiroplasma* in *Myrmica* queens and workers and uncovered how *Ixodetis* variants co-segregate with *Citri* variants. By establishing and genome-sequencing 10 monogynous experimental colonies, we were now able to characterize the toxin repertoires of specific *Myrmica*-associated *Spiroplasma* variants and test for co-cladogenesis of *Spiroplasma* and *Myrmica*.

2 | Material and Methods

2.1 | 16S rRNA Long-Read Amplicon Sequencing of *Myrmica* Queens

From seven *Myrmica* species, 20 queens were isolated from 18 field colonies, preserved in ~95% ethanol and stored at 4°C until DNA extraction (Table S1). DNA was extracted from the *Myrmica* queens using the Quick-DNA Universal kit (BaseClear, the Netherlands) (Figure 1). Full-length 16S rRNA genes were amplified and prepared for amplicon sequencing using two PCR rounds (Table S2). Pooled DNA was purified with the AMPure XP system. Pooled libraries were prepared for the Nanopore Flongle cell chemistry R10.4.1 using the SQK-LSK114 kit with Amplicon by ligation protocol. Basecalling was performed with Dorado 0.8.1 using the super-accurate option. A quality read threshold of 15 was implemented for the read output. Raw reads were demultiplexed and adapters trimmed using a custom python script (<https://github.com/avierstr/umipore>). Consensus sequences for each library were created with amplicon_sorter using a 99% threshold of similarity (Vierstraete and Braeckman 2022). With the consensus sequence information (number of contributing sequences), we denoised each sample separately, followed by chimera removal, OTU-clustering and taxonomic classification against the SILVA database (v.138) using USEARCH and VSEARCH (Edgar 2010; Quast et al. 2012; Rognes et al. 2016). The final OTU table was generated using a minimum read number threshold of 50.

2.2 | Metagenome Sequencing and Assembly From Monogynous Colonies

Natural *Myrmica* colonies are typically polygynous, resulting in multiple maternal lineages within a single field colony. We therefore established experimental monogynous colonies in the laboratory to confirm and further dissect infection heterogeneity in *Myrmica* ants. We sampled a total of 10 new field colonies from six *Myrmica* species and isolated a single queen from each field colony. We were unable to locate a new field colony of *M. schencki*. To study co-infection of *Citri Spiroplasma* in more detail in *M. ruginodis* and *M. sabuleti* (Figure 1), three and two field colonies were sampled, respectively. For *M. rubra*, two field colonies were sampled, whereas a single field colony was sampled for the remaining three *Myrmica* species (*rugulosa*, *specioides* and *scabrinodis*). Each experimental colony was initiated using a single queen and was given the label My-1 to My-10 (Supporting Information S1). After 4 months, we collected the queen, pupae and new callow workers, all belonging to a single maternal lineage. DNA was extracted using the Quick-DNA Universal kit (BaseClear, the Netherlands) and was sequenced on a Novaseq Illumina platform (Fasteris, Switzerland) (Table S1). Read

quality was verified using FastQC v0.11.9 (<https://github.com/s-andrews/FastQC>). Contigs were assembled using Megahit v1.2.9 (maximum k-mer size=255 and min contig size=1000) (Li et al. 2015). Reads were mapped against the assembled contigs using bowtie2 (Langmead and Salzberg 2012). SAM files were sorted and converted to BAM using samtools v1.19.2. To overcome the challenges of low infection density in the My-10 colony, reads were mapped against the *Spiroplasma* assembly of My-1 using bowtie2. SAM files were converted to fastq using samtools v1.21 and the paired-end files were generated using Bbmap tools (<https://github.com/BioInfoTools/BBMap/>). A final assembly was generated using Megahit v1.2.9 (Li et al. 2015). Using the same pipeline as described above, new metagenome assemblies were generated from two DNA samples from a previous study (from *Myrmica scabrinodis* and *Myrmica vandeli*) (Ballinger et al. 2018).

2.3 | *Spiroplasma* Binning and Classification From Monogynous Colonies

The taxonomic composition of the *Myrmica* microbial communities was assessed with 16S rRNA and 18S rRNA sequences using PhyloFlash v3.4 (Gruber-Vodicka et al. 2020). Using anvi'o, metagenome assemblies were further processed by contig reformatting, anvi'o database creation and running anvi-get-sequences-for-hmm-hits to identify rRNA sequence-containing contigs (Eren et al. 2015). Nuclear, mitochondrial and prokaryotic contigs were identified using NanoTax.py (<https://github.com/diecasfranco/Nanotax>). *Spiroplasma* bins were recovered from the metagenome assemblies using CONCOCT, MaxBin2 v2.2.5, MetaBAT2 v2.12.1 and Metadecoder v.1.0.19 (Alneberg et al. 2014; Kang et al. 2019; Liu et al. 2022; Wu et al. 2016). Optimal binning was identified by contrasting the bins using DAS Tool v1.1.0 (Sieber et al. 2018). In parallel, we extracted contigs taxonomically classified as *Spiroplasma* using BLASTn searches against NCBI nt database (dated March 2024). Completeness and contamination of the *Spiroplasma* bins was assessed with CheckM2 v1.0.2 (--allmodels and --ttable 4) and BUSCO v6.0.0 (using the spiroplasma_odb12 dataset) (Chklovski et al. 2023; Seppey et al. 2019). *Spiroplasma* bins were classified taxonomically using GTDB-Tk v2.3.2 (Chaumeil et al. 2022). Average nucleotide identity (ANI) was calculated using the anvi-compute-genome-similarity script (--program pyANI, option ANIb) (Eren et al. 2015). *Spiroplasma* genomes, including public reference genomes, were annotated using prokka v.1.14.6 (--gcode 4 and --compliant) (Seemann 2014) (Table S3). Orthologous gene families of the focal *Spiroplasma* genomes were classified using OrthoFinder v2.5.5. Protein sequences of single-copy orthologs were aligned with MAFFT v7.520 and concatenated (Kato and Standley 2013). IQ-Tree2 was used to generate the phylogenetic tree (-m MFP+MERGE -B 5000 --alrt 1000) (Minh et al. 2020).

2.4 | Spread of *Spiroplasma* and *Wolbachia* in Myrmicini Workers

To study (co-)infection of symbionts in Myrmicini workers, a total of 60 *Myrmica* colonies and three *Manica* colonies were field-sampled across several European countries between 2020

and 2024 (Table S1). Both the queen and worker caste were genotyped for *Spiroplasma* and *Wolbachia* infection for a total of 16 *Myrmica* colonies (Table S1). Workers were isolated from field colonies, preserved in ~95% ethanol and stored at 4°C. DNA was extracted using the Quick-DNA Universal kit (BaseClear, the Netherlands). To resolve the species identity for all field colonies, we followed the morphological keys of Seifert (2007). For a subset of 27 Myrmicini colonies, DNA extracts were used to validate our morphological species classification by *COI* sequencing (Tables S1 and S2). A maximum-likelihood phylogeny using seven reference *COI* fragments was constructed using IQ-Tree2 (ModelFinder, ultrafast bootstrapping with 10,000 replications) (Minh et al. 2020). To estimate the spread of *Ixodetis* and *Citri Spiroplasma* as well as *Wolbachia* in Myrmicini workers, end-point diagnostic PCR assays were performed on 368 field-collected workers (Tables S1 and S2). We tested whether the infection frequency of *Citri* and *Ixodetis Spiroplasma* differed significantly within individual workers of the *scabrinodis* and *rubra* species groups by performing a McNemar's chi-squared test with continuity correction separately for each species group. We subsequently tested whether colonies from the *rubra* species group exhibited significantly different infection frequencies of *Ixodetis Spiroplasma* compared to those from the *scabrinodis* species group. Here, a beta-binomial model was fitted using the *glmTMB* package, with the proportion of *Ixodetis*-infected workers per colony as the response variable and species group as a fixed effect. Model diagnostics using the *DHARMA* package indicated no violations of model assumptions. Finally, we tested whether infection of *Citri* and *Ixodetis Spiroplasma* and *Wolbachia* co-occurred more often than expected by chance. Pairwise associations between symbionts (*Citri*–*Ixodetis*, *Citri*–*Wolbachia* and *Ixodetis*–*Wolbachia*) were evaluated in the *scabrinodis* and *rubra* species groups using six Fisher's exact tests.

Infection frequencies of *sRug1* and *sRug2* of *M. ruginodis* workers were quantified by two-way Sanger sequencing of PCR amplicons from 51 workers (across 18 field colonies). Sanger trace data was investigated at 18 polymorphic sites at the *ftsZ* locus (MACROGEN Europe B.V., Tables S1, S2 and S4). For this subset of 51 workers, we tested whether the infection frequency of *sRug1* and *sRug2* differed significantly within individuals using McNemar's chi-squared test with continuity correction. To study the tissue specificity of *Citri Spiroplasma*, adult workers from *M. ruginodis* were dissected. Tissue types (head, mesosoma, gaster and legs) were pooled per two to three workers and four samples were tested using end-point diagnostic PCR (Table S2). Infection heterogeneity was tested for one Sanger-sequenced gaster sample using 18 polymorphic sites at the *ftsZ* locus (Table S4).

2.5 | Acquisition Mode of *sMyr Spiroplasma* in European *Myrmica*

To experimentally demonstrate maternal transmission of *sMyr Spiroplasma*, 11 eggs of the *My-1 M. scabrinodis* queen were collected and preserved in ~95% ethanol at –20°C. Egg morphology was investigated to ensure no trophic eggs were included. Two eggs were surface-sterilized through a 30s immersion in 1% bleach, followed by four rounds of washing for 1 min in sterile water. DNA was extracted from individual eggs using the

Quick-DNA Universal kit with Elution Buffer pre-equilibrated to 60°C (BaseClear, the Netherlands). End-point diagnostic PCR assays were performed to test for infection of *sScab2*, *sMyr* and *Wolbachia* (Tables S1 and S2).

Using the 10 metagenomes of monogynous colonies, circular mitochondrial genomes were annotated with MitoZ v3 (–clade Arthropoda) (Meng et al. 2019). The 13 mitochondrial nucleotide and protein sequences were aligned using MAFFT v7.520 (Katoh and Standley 2013). Single-copy orthologs of the 6 *sMyr* isolates and *S. melliferum* outgroup were identified and aligned using OrthoFinder v.2.5.5 and MAFFT v7.520, respectively (Katoh and Standley 2013). After alignment concatenation, three maximum-likelihood phylogenetic reconstructions were generated using IQ-Tree2 (–m MFP+MERGE –B 5000 –alrt 1000), MrBayes (ModelTest-NG v0.1.7 and 100,000 generations) and RaxML v.8.2.12 (–p 35 –x 345 –#500 –m PROTGAMMAWAG).

To generate a time-calibrated nuclear phylogenetic reconstruction of *Myrmica*, we used genomic resources of *Pogonomyrmex barbatus* and *Acromyrmex echinator* as outgroups (Nygaard et al. 2011; Smith et al. 2011). Single-copy orthologs were retrieved from the genome assemblies using BUSCO with the *hymenoptera_odb10* database and the *augustus_species* option set to *Camponotus floridanus* (Seppey et al. 2019) and were aligned with MAFFT (Katoh and Standley 2013). We concatenated the 5887 nuclear genes and performed a phylogenetic analysis with IQ-Tree2, using a GTR+I+F+G4 partition model for each gene and 1000 ultrafast bootstraps. To generate a time-calibrated mitochondrial phylogenetic reconstruction of *Myrmica*, we used the mitochondrion sequences of *Acromyrmex octospinosus* (BK012808.1) and *Pogonomyrmex occidentalis* (BK012408.1) as outgroups. Dated phylogenies from the two trees and corresponding alignments were produced using rapid approximate likelihood computation of MCMCtree from the PAML package (Yang 2007). Trees were calibrated using data from (Romiguier et al. 2022), for the node grouping *Myrmica* and *Pogonomyrmex* (between –59.4 and –79.6 Myrs) and the node grouping *Myrmica* and *Acromyrmex* (between –67.4 and –86.8 Myrs). We performed two runs of the correlated rates model, HKY85 substitution model for 30 million generations. We confirmed convergence and sufficient effective sample sizes (>> 200) for all parameters using Tracer (Rambaut et al. 2018).

2.6 | Functional Prediction of *Spiroplasma* Transmission and Phenotypes in *Myrmica*

RIP, OTU, ankyrin and ETX/MTX2 protein domains were identified in the *Spiroplasma* genomes from *Myrmica* using a curated database (Moore and Ballinger 2023). Specifically, HMM profiles were created for each toxin. Using *hmmsearch*, we identified candidate toxins in each *Spiroplasma* genome using a threshold e-value of E-10 (Eddy 2011; Finn et al. 2011). Final sets of candidate *Spiroplasma* toxins were retrieved after domain confirmation using InterProScan and HHpred (Hildebrand et al. 2009; Jones et al. 2014). Protein sequences were aligned using MAFFT. Phylogenies were built using IQ-Tree2 (v.2.2.6) (–m MFP+MERGE –B 5000 –alrt 1000), RAXML (v.8.2.12) (–p 35 –x 345 –#500 –m PROTGAMMAWAG) and MrBayes (best model identified via ModelTest-NG v0.1.7 and 100,000

generations) (Minh et al. 2020; Ronquist and Huelsenbeck 2003; Stamatakis 2014). Our genome-sequenced *Spiroplasma* and *Wolbachia* variants were also surveyed for *cif* genes that may underlie CI (Supporting Information S1). Our *Spiroplasma* genomes were further screened for CRISPR/Cas arrays using CRISPRCasFinder v4.2.20 (Couvin et al. 2018). Nucleotide and protein sequences were annotated using Interproscan (Jones et al. 2014). Prophage regions were identified using PHASTEST (Wishart et al. 2023), PhiSpy v.4.2.21 (Akhter et al. 2012) and Phigaro v.2.3.0 (Starikova et al. 2020).

To characterize unique and enriched metabolic features of sMyr *Spiroplasma*, two *Spiroplasma* genome panels were used to create anvi'o databases and were annotated using KEGG, COG and Pfam (Eren et al. 2015) (Table S3). The first panel consisted of variants across the *Spiroplasma* group, whereas the second panel was strictly comprised of Citri representatives. We used the anvi-pan-genome script (default parameters) and identified gene clusters based on amino acid sequence similarity. Functional enrichment was identified using anvi-compute-functional-enrichment-in-pan, contrasting the six sMyr isolates against the rest of the two genome panels (Pfam, Kofam, COG20_FUNCTION and COG20_PATHWAY). The anvi-display-pan script was used to visualize the gene cluster distribution.

3 | Results

3.1 | Multiple Cryptic *Spiroplasma* Co-Infections Typify *Myrmica*

To test for co-infection of *Spiroplasma* in *Myrmica*, we first characterized the symbiotic community of 20 field-collected *Myrmica* queens (belonging to seven species) using a 16S rRNA amplicon long-read sequencing approach. We obtained a total of 81,444 reads, ranging in size between 1400 and 1498 bp (average read length was 1438.7 bp). We detected 12 Operational Taxonomic Units (OTUs) across the *Myrmica* queens (Figure S1,

Table S5). Taxonomic classification of these OTUs revealed that a total of three queens carried Ixodetis *Spiroplasma* (2/5 of *M. scabrinodis* and 1/1 of *M. specioides*, Figure 1). This finding contrasts with a previous survey that did not detect Ixodetis *Spiroplasma* in *Myrmica*, a discrepancy that is likely caused by the clade-specificity of its diagnostic assay (Figures S2 and S3, Table S2) (Ballinger et al. 2018; Haselkorn et al. 2009). OTU classification further revealed that two Citri variants infected all four *M. ruginodis* queens. One of two *M. sabuleti* queens also carried two Citri variants. *M. scabrinodis* and *M. rubra* carried *Wolbachia* symbionts (5/5 and 4/5 queens were infected, respectively) (Figure 1).

To further study and characterize the genomes of co-infecting *Spiroplasma* variants in *Myrmica*, we isolated single queens from new field colonies and established experimental monogynous colonies. One field colony was sampled for *M. scabrinodis*, *M. specioides* and *M. ruginodis*. Two field colonies were sampled for *M. rubra*. As *M. ruginodis* and *M. sabuleti* queens displayed noteworthy Citri co-infections (Figure 1), we increased our sampling efforts to three and two field colonies, respectively. We generated Illumina short-read data at high sequencing depth from these experimental monogynous colonies (My-1 to My-10) (Figure 2). Metagenome assembly, curated binning and taxon-annotated GC/coverage plots showed that nine of the 10 experimental colonies exhibited signatures of *Spiroplasma* infection (Figure 2, Figures S2 and S4, Tables S1 and S6). The My-7 *M. ruginodis* colony did not appear to carry *Spiroplasma*, a finding that was consistent with diagnostic PCR assays on five additional workers. Leveraging *Myrmica* host, ANI values and phylogenetic placement, we clustered certain *Spiroplasma* isolates to a single variant ID (Figure 2). For the nine infected experimental colonies, the size of the fragmented *Spiroplasma* genome assemblies ranged between 450,834 bp (sRug1 from My-8) and 2,501,504 bp (sSabu2 from My-4) (Figure 2, Table S6). Bin completeness was assessed using two approaches and showed that the quality of our fragmented *Spiroplasma* genome assemblies is in line with reference

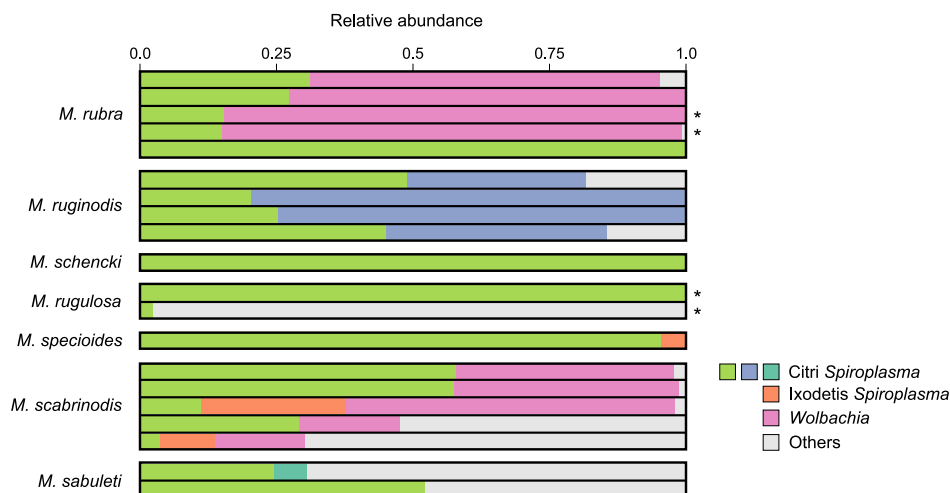


FIGURE 1 | Citri and Ixodetis *Spiroplasma* co-infections typify *Myrmica* queens. For seven *Myrmica* species, each row represents the relative abundance of *Spiroplasma* and *Wolbachia* in a single field-collected queen. Queens that are highlighted with an asterisk were isolated from the same field colony. Otherwise, each queen was isolated from a unique field colony (Figure S1, Table S1). The 20 queen microbiomes are characterized by 16S rRNA long-read amplicon sequencing. OTUs were identified using a 99% threshold of similarity. A total of four *Spiroplasma* OTUs (including Citri and Ixodetis) were identified and were often found co-infecting *Myrmica* queens.

genomes (Table S6). Binning, ANI analyses, whole-genome- and 16S rRNA-based phylogenetic approaches confirmed that *M. scabrinodis* and *M. specioides* carry Ixodetis *Spiroplasma* (sScab2 and sSpec2, respectively) (Figure 2, Figures S2 and S5, Table S3). Together, these results show that Ixodetis *Spiroplasma* are cryptic symbionts in *Myrmica*, undetected in previous surveys (Ballinger et al. 2018) (Figure S3).

Consistent with the 16S rRNA amplicon sequence analysis (Figure 1), binning, ANI analyses and whole-genome- and 16S

rRNA-based phylogenetic reconstruction uncovered that the My-5 and My-8 *M. ruginodis* colonies carried a co-infection of Citri variants (Figure 2, Figures S2 and S5). These variants display an ANI value of ~0.86, are polyphyletic and are hereafter referred to as sRug1 and sRug2 (Figure 2, Figures S2 and S5). Maximum-likelihood phylogenetic reconstruction of the 14 *Spiroplasma* isolates from our monogynous colonies uncovered that a certain variant, hereafter referred to as sMyr, was found in four *Myrmica* species (*M. rugulosa*, *M. specioides*, *M. sabuleti* and *M. scabrinodis*) (Figure 2). To clarify, whereas previous work described the *Spiroplasma* variant of *M. scabrinodis* as sScab (Ballinger et al. 2018; Moore and Ballinger 2023), we propose the name sMyr considering its spread across multiple *Myrmica* species (see also further sections of this study). The phylogenetic reconstruction further placed sRug1 with sMyr (Figure 2). While metagenome binning revealed that the My-3 *M. sabuleti* colony was infected with a single isolate from sMyr, the My-4 *M. sabuleti* colony carried an additional Citri variant, sSabu2 (Figure 2, Figure S2). The phylogenetic analysis grouped sRug2 and sSabu2 together (Figure 2). Finally, our analyses also showed that *Wolbachia* infected the My-1 *M. scabrinodis* colony (Table S7).

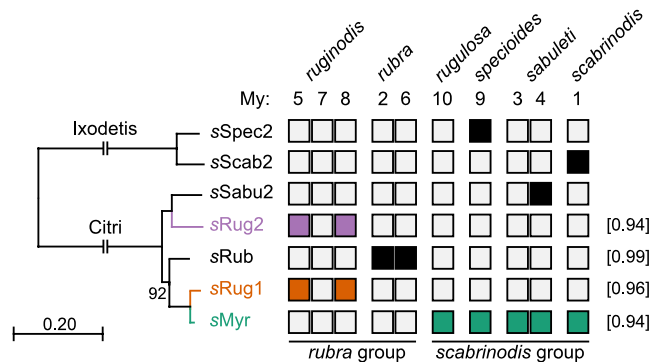


FIGURE 2 | Distinct variants of Citri *Spiroplasma* co-infect monogynous colonies of *Myrmica*. Phylogeny shows the seven *Spiroplasma* variants that were identified in our panel of *Myrmica* metagenomes. Metagenomes were generated using experimental monogynous colonies (My-1 to My-10). Maximum-likelihood phylogeny was constructed with 27 single-copy orthologs. No support values are depicted when the maximum-likelihood approach identified a support value of 100. For each *Spiroplasma* variant with several sequenced genomes, the lowest ANI value is provided within squared brackets. Two *M. ruginodis* colonies carried a sRug1 and sRug2 co-infection. sMyr was identified in five samples of four *Myrmica* species. We also identified sMyr in a metagenome sample from a previous study (Ballinger et al. 2018). Figure S2 depicts an ANI heatmap of *Myrmica*-associated and reference *Spiroplasma* genomes.

3.2 | Ixodetis *Spiroplasma* Segregate at Lower Frequencies Compared to Citri *Spiroplasma* in *Myrmica* Workers

To study *Spiroplasma* (co-)infection in Myrmicini workers, we sampled 368 workers from 63 field colonies (Figure 3, Table S1). For 16 field colonies, both the queen and worker castes were genotyped for *Spiroplasma* and *Wolbachia* infection (Table S1). Morphological classification revealed that our worker panel consisted of six *Myrmica* species (*rubra*, *ruginodis*, *rugulosa*, *specioides*, *sabuleti* and *scabrinodis*). Maximum-likelihood phylogeny using a *COI* fragment of 27 field colonies was consistent with this species classification (Figure S6). The phylogeny further revealed that workers from both the mitochondrial A- and B-group of *M. scabrinodis* were sampled and

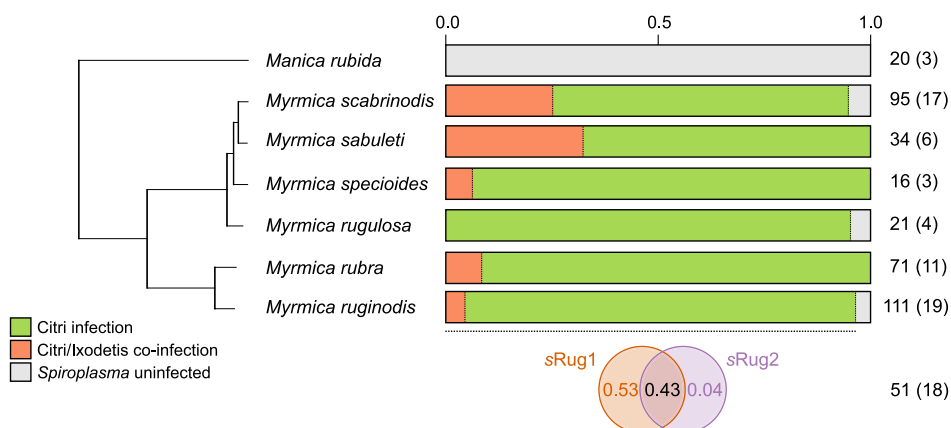


FIGURE 3 | Citri and Ixodetis *Spiroplasma* display variable infection frequencies in *Myrmica* workers. Mitochondrial phylogeny shows (co-)infection patterns of Citri and Ixodetis *Spiroplasma* across six *Myrmica* species and *Manica rubida*. Number of sampled workers and colonies are delineated, with colony number within brackets. For *M. ruginodis* workers, the infection frequencies of sRug1 and sRug2 are further outlined. Sanger trace data showed that the infection of both Citri variants is not fixed, generating four infection states in *M. ruginodis* workers. Infection frequency of sRug1 is significantly higher in workers compared to sRug2.

were hereafter analysed together (Figure 3, Figure S6) (Ebsen et al. 2019).

Within our *Myrmica* worker panel, Citri *Spiroplasma* reached near-fixation frequencies, ranging between 0.947 and 1.000. In contrast, using a newly developed diagnostic assay (Figure S3), our survey revealed that Ixodetis *Spiroplasma* exhibited lower and more variable infection frequencies across *Myrmica* species (Figure 3). Whereas *M. rugulosa* did not show signs of infection, Ixodetis *Spiroplasma* displayed an infection frequency between 0.045 and 0.324 in the other *Myrmica* species (Figure 3). *Myrmica* workers from both the *scabrinodis* and *rubra* species groups showed a significantly higher infection frequency of Citri *Spiroplasma* compared to Ixodetis, as indicated by McNemar's chi-squared tests (*scabrinodis* species group: $\chi^2=122.01$, $df=1$, $p<0.001$; *rubra* species group: $\chi^2=165.01$, $df=1$, $p<0.001$). However, colonies of the *scabrinodis* and *rubra* species groups did not significantly differ in the infection frequency of Ixodetis *Spiroplasma* ($\chi^2=2.28$, $df=1$, $p=0.131$). *Wolbachia* symbionts were identified in *M. scabrinodis*, *M. sabuleti* and *M. rubra*, with infection frequencies ranging between 0.268 and 0.779 (Figure S7). We found no evidence that Citri and Ixodetis *Spiroplasma* and *Wolbachia* co-occurred at the individual worker level more often than expected by chance (all six p -values >0.18). The statistical analysis of co-infection was likely constrained by the low variability in Citri *Spiroplasma* infection, which was present in nearly all *Myrmica* workers. As an outgroup, morphological and molecular classification showed that we collected 20 *Manica rubida* workers. None of the *M. rubida* workers carried *Spiroplasma* or *Wolbachia* symbionts (Figure 3, Figure S7).

3.3 | Infection Frequency of sRug2 is Contingent on Ant Caste

Two Citri variants, sRug1 and sRug2, were observed in queens and colonies of *M. ruginodis* (Figures 1 and 2). Here, four additional field-collected *M. ruginodis* queens were Sanger genotyped and were infected with sRug1 and sRug2 (Table S1, Figure S8). To study the infection frequency of sRug1 and sRug2 in individual *M. ruginodis* workers, we genotyped the Citri infection profile of 51 field-collected workers by Sanger sequencing. These genotyping efforts showed that four infection states exist in *M. ruginodis* workers, albeit at divergent frequencies. Whereas ~96% of infected workers carried sRug1, only ~47% were infected with sRug2 (Figure 3, Figure S8). Infected *M. ruginodis* workers were significantly more likely to carry sRug1 than sRug2 ($\chi^2=19.862$, $df=1$, $p<0.001$). Together, our results suggest that the Citri co-infection is widespread in *M. ruginodis* queens (10/11 tested positive) and that sRug2 exhibited an infection bias towards *M. ruginodis* queens (Table S1). To study the tissue specificity of sRug1 and sRug2, head, mesosoma, gaster and legs were dissected from pooled *M. ruginodis* samples. All four gaster samples tested positive. Sanger sequencing of a pooled gaster sample revealed a single infection of sRug1. For both the mesosoma and head, two samples tested positive for Citri infection. None of the leg samples were positive.

3.4 | Evidence for Cladogenic Acquisition of sMyr Spiroplasma Across Four Myrmica Species

Infection of sMyr in four European *Myrmica* species can be explained by three potential transmission routes: horizontal non-sexual transmission across host species, interspecific hybridization followed by introgression, or by cladogenic acquisition. A prerequisite for cladogenic acquisition is the ability of sMyr to maternally transmit. We experimentally verified maternal transmission by genotyping 11 eggs of the My-1 *M. scabrinodis* queen that was infected with sMyr and sScab2 *Spiroplasma* and *Wolbachia* (Figure 2). All eggs, including two samples that were surface-sterilized, tested positive for sMyr and *Wolbachia*. Only three eggs appeared to carry sScab2 and were not surface-sterilized (Table S1). These results indicate that sMyr *Spiroplasma* and *Wolbachia* have a (near-)perfect maternal transmission efficiency in *M. scabrinodis*.

To further investigate the transmission route(s) of sMyr, we generated new draft *Spiroplasma* genomes from a *M. scabrinodis* and a *M. vandeli* metagenome sample from a previous study (Ballinger et al. 2018). Characterization of mtDNA revealed that two mitochondria were segregating in the *M. vandeli* sample, suggesting that the field-collected workers were derived from different *M. vandeli* queens, a likely scenario considering that *Myrmica* colonies are typically polygynous (Supporting Information S1). No strong evidence was collected for multiple mitochondria in the *M. scabrinodis* sample and metagenome binning generated a single draft *Spiroplasma* genome (Figure 4A, Figure S2). Circular mitochondrial genomes were recovered from the *Myrmica* host species (size ranged between 15,451 and 15,678 bp for the monogynous colony panel).

Using three different maximum-likelihood approaches and 258 single-copy orthologs, the topologies of the six sMyr isolates and *Myrmica* mitochondria were recurrently congruent (Figure 4A). Phylogenetic congruence between sMyr and *Myrmica* mitochondria persisted after removing the sMyr genome isolated from the previously sequenced *M. scabrinodis* field colony (Figure S9A) (Ballinger et al. 2018). This phylogenetic congruence suggests joint maternal transmission of sMyr and mitochondria, arguing against horizontal non-sexual transmission between these *Myrmica* species of the *scabrinodis* group. To test for recent interspecific introgression of mitochondria across these four *Myrmica* species, we contrasted the topologies and estimated divergence times of nDNA and mtDNA (Figure 4B, Figure S9B). The age of the most recent common ancestor (MRCAs) of the four *Myrmica* species was roughly equal for nDNA and mtDNA, dating to 7.40 and 6.58 MYA, respectively (Figure 4B, Figure S9B). Topologies were identical, except that the nDNA topology shows that *M. specioides* and *M. rugulosa* are sister lineages, suggestive of some level of interspecific hybridisation while retaining both ancestral mtDNA variants (Figure 4B, Figure S9B). Together, our results currently favour cladogenic acquisition of sMyr *Spiroplasma*. However, the high similarity between the sMyr variants (lowest ANI value was ~0.94) raises questions about the interpretation of these results as cladogenic acquisition (Figures 2 and 4, Figure S2), considerations that are discussed in more detail later.

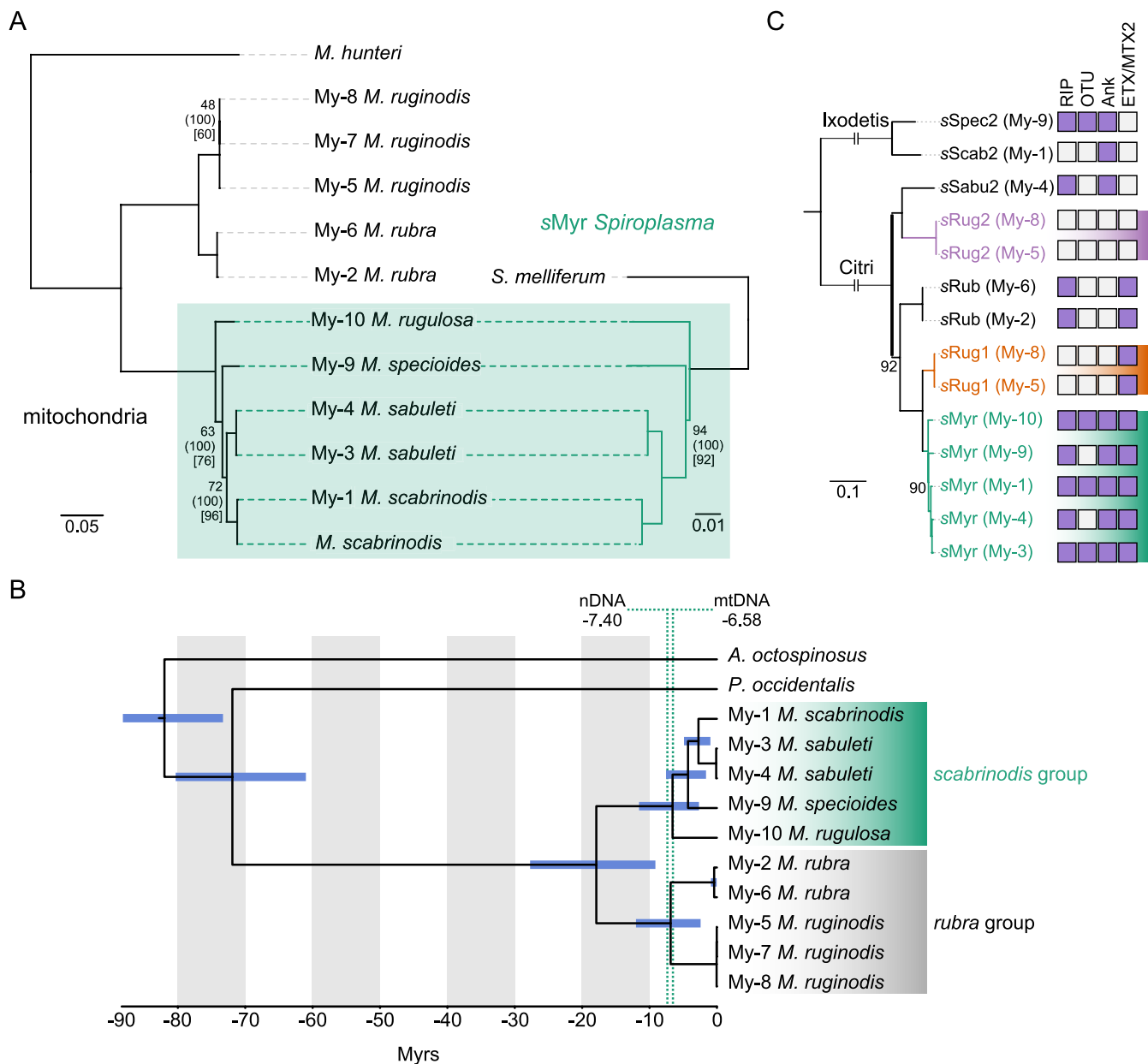


FIGURE 4 | Phylogenomic evidence for a seven-million-year infection of sMyr *Spiroplasma* in *Myrmica* ants. Panel (A) shows the congruent phylogeny of mitochondria and sMyr within four *Myrmica* species. sMyr phylogeny was rooted with *S. melliferum*, whereas *Myrmica* phylogeny was rooted with a *M. hunteri* mitochondrion. No support values are depicted when all three maximum-likelihood approaches identified a support value of 100. Values from IQ-Tree2, MrBayes and RaxML are shown without brackets, within round brackets, and within squared brackets. The *M. scabrinodis* lineage without a My-ID is derived from a previous study (Figure S9) (Ballinger et al. 2018). Panel (B) shows the time-calibrated mitochondrial phylogeny of the focal *Myrmica* species using *A. octospinosus* and *P. occidentalis* as outgroups. Age of the MRCA of the sMyr-infected *Myrmica* species group is estimated based on the mitochondrial and nuclear sequence data (Figure S9). Panel (C) shows the toxin repertoire of the 14 genome-sequenced *Myrmica*-associated *Spiroplasma* isolates. Maximum-likelihood phylogeny was constructed with 27 single-copy orthologs.

3.5 | Genomic Support for Stable Maternal Transmission as the Main Acquisition Mode of sMyr

To further study sMyr *Spiroplasma* symbiosis in *Myrmica*, we identified absent and enriched metabolic features encoded by sMyr genomes by performing metabolic enrichment analyses using two different genome reference panels (Tables S8–S15). The first reference panel consisted of genomes sampled across the *Spiroplasma* group, whereas the second panel was strictly

comprised of Citri representatives. Using single-copy orthologs, a phylogenomic reconstruction of sMyr and the Citri-specific panel confirmed our previous observations that sRug1 appears as a related lineage of sMyr (Figures S2, S5 and S10). Using a *p*-value threshold of 0.05 and the genus-wide reference panel, between 6 and 86 terms were significantly enriched in *Spiroplasma* genomes compared to sMyr. With the COG20_PATHWAY analysis, a number of biosynthetic pathways were identified, including lipoate and pyridoxal phosphate biosynthesis. Pfam enrichment identified a significant absence of the thiamine

biosynthesis protein (ThiI, PF02568) in sMyr (Table S8). This apparent metabolic reduction of sMyr in thiamine biosynthesis was also observed in the enrichment analyses using the Citri-specific reference panel (Table S12). KEGG annotations however revealed that thiamine, lipoate and pyridoxal phosphate biosynthesis are typically not complete in *Spiroplasma* genomes, suggesting that a reduced biosynthetic ability is not a unique feature of sMyr. Consistent with previous work on the Citri clade, the CRISPR-CAS system was enriched in the genus-wide genome panel compared to sMyr (Table S8) (Gerth et al. 2021).

Using the genus-wide reference panel, enrichment analyses further identified between 2 and 43 terms that have a significant enrichment in sMyr compared to other *Spiroplasma* genomes (with a *p*-value threshold of 0.05). Of note, Pfam enrichment uncovered OTU-like cysteine protease and ankyrin repeats as significant features of sMyr *Spiroplasma* (PF02338 and PF13637, respectively). Ankyrin repeats were also enriched in sMyr using the Citri-specific reference panel (Table S12). Interestingly, previous work uncovered a strong association between these protein domains and maternal transmission in *Spiroplasma* (Moore and Ballinger 2023). *spaid* of sMel *Spiroplasma* controls MK and encodes ankyrin repeats and an OTU deubiquitinase domain (Harumoto and Lemaitre 2018). Subsequent HMMER searches confirmed that three sMyr isolates (from the My-1, My-3 and My-10 colonies) and sSpec2 encode an OTU-containing protein (Figure 4C, Figure S11). Previous work also uncovered a link between the RIP domain and maternal transmission (Moore and Ballinger 2023). RIPs mediate protection against parasitic wasps and nematodes in insects (Ballinger and Perlman 2017, 2019). Although both Pfam and HMMER searches uncovered RIP domains in all sMyr variants (PF00161), no significant enrichment was observed. A total of 14 candidate RIPs were identified in *Myrmica*-associated *Spiroplasma* (Figure S11), a finding that is consistent with previous work (Ballinger et al. 2018; Moore and Ballinger 2023). Three sMyr isolates (from the My-1, My-3 and My-9 colonies) encoded for two adjacent candidate RIP genes (Figure S11), with sMyr from the My-3 colony coding for a third candidate RIP paralog (Figure S11). The other two sMyr isolates from the My-4 and My-10 colony encoded two and one candidate RIP, respectively. In addition, sSabu2, sSpec2 and sRub also encoded for a single candidate RIP. Consistent with previous studies, a great phylogenetic diversity of candidate RIPs was found in *Spiroplasma* of *Myrmica* (Figure S11). An additional association between maternal transmission in *Spiroplasma* and protein domains was found for ETX/MTX2 toxins (Moar et al. 2017; Moore and Ballinger 2023; Palma et al. 2014) (Figure 4C). Of note, none of these toxin domains were uncovered in sRug2 *Spiroplasma* (Figure 4C). Finally, several Pfam terms related to prophages were significantly enriched in sMyr using the genus-wide reference panel (e.g., PF04883 and PF06488) (Table S8). These enrichment results support the negative association of CRISPR/Cas systems and prophage proliferation in Citri *Spiroplasma* (Gerth et al. 2021).

To better understand whether CI may promote the spread of *Spiroplasma* and *Wolbachia* in *Myrmica* ants, we surveyed our genome-sequenced variants for the presence of *cif* genes. No functional *cifA;B* gene pairs were identified in our 14 *Myrmica*-associated *Spiroplasma* genomes. Using our survey thresholds, a single apparent functional *cif* pair was identified in the genome

of the *Wolbachia* variant that infects the My-1 *M. scabrinodis* colony. Maximum-likelihood phylogeny places this *cif* pair within Type I, a group of enzymes with a functionally validated role in CI (Figure S12) (LePage et al. 2017; Martinez et al. 2021).

4 | Discussion

Infections of facultative maternally transmitted symbionts typically do not persist on the same timescale as insect speciation. Loss of infection is expected to be compensated by horizontal (non-maternal) transmission across host species, especially for *Spiroplasma*, a symbiont with an intra/extracellular lifestyle (Herren et al. 2013; Sanaei et al. 2021). As a result, phylogenies of *Spiroplasma* and mitochondria of insect hosts are not congruent (Haselkorn et al. 2009). Here, we uncover strong congruence between *Myrmica* mitochondria and sMyr *Spiroplasma* across six samples of four species (*scabrinodis*, *sabuleti*, *specioides* and *rugulosa*). This phylogenomic pattern is consistent with the previously suggested trend of co-cladogenesis between *Spiroplasma* and *Myrmica* (Ballinger et al. 2018) and now presents evidence that sMyr *Spiroplasma* colonized an ancestral host of the *scabrinodis* species group seven million years ago.

However, horizontal transmission between closely related and/or sympatric host species may also generate phylogenetic congruence (De Vienne et al. 2007). As all queens that founded the 10 experimental colonies were collected within the provinces of East and West Flanders (Belgium), geographic distribution does not easily explain the infection pattern of sMyr across all six *Myrmica* species. Moreover, the second *M. scabrinodis* sample originated from France and clustered with our My-1 *M. scabrinodis* colony (Ballinger et al. 2018). Horizontal transfer of large genomic fragments from symbiont into the host nuclear genome could also explain phylogenetic congruence. However, our taxon-annotated coverage plots show clear divergent levels of coverage between *Myrmica* and sMyr scaffolds. Moreover, six field-collected *Myrmica* workers apparently lost sMyr infection. These findings do not support a horizontal genome transfer event. A formal test of cladogenic acquisition of symbionts is to verify whether the divergence times of host and symbiont align. Here, the high nucleotide similarity between the sMyr variants challenges our interpretation of the results, especially considering *Spiroplasma* is a fast evolving symbiont in certain host species (Gerth et al. 2021). There are several constraints that currently prevent a reliable estimate of mutation rate and divergence time of sMyr in *Myrmica* ants. *Myrmica* queens are produced seasonally and exhibit reproductive lifespans of ~2 years, creating variable numbers of generations across regions and species (Evans 1996; Pedersen and Boomsma 1999). Moreover, presence of co-infecting *Spiroplasma* variants such as sSpec2, sScab2 and sSabu2 as well as potential plasmids in the metagenome samples complicate reliable variant calling for sMyr, further hindering accurate estimates of mutation rate and divergence time (Gerth et al. 2021). We further acknowledge that our interpretation of a cladogenic spread of sMyr would benefit from additional species sampling within the *scabrinodis* group. Phylogenetics of *Myrmica* mitochondria places additional species, including *Myrmica hellenica*, within this sMyr-infected species group, highlighting certain host species as interesting targets for future *Spiroplasma* surveys (Ebsen et al. 2019). In

parallel, future studies should also be directed towards unravelling close relatives of sMyr *Spiroplasma* that might infect other insect genera and species.

Cladogenic acquisition of symbionts has been observed in other ant lineages (Cabuslay et al. 2024; Degnan et al. 2004; Hu et al. 2023; Jackson et al. 2022), including the *Camponotus* and *Cardiocondyla* genera that acquired *Blochmannia* and *Westeberhardia* bacteria ~40 and 50–75 million years ago, respectively (Degnan et al. 2004; Jackson et al. 2022). Here, the exceptional stability of these symbioses is likely facilitated by the intracellular localization and nutrient provisioning by these bacteria (Degnan et al. 2004; Jackson et al. 2022; Klein et al. 2016; Moreau et al. 2006; Schröder et al. 1996; Williams and Wernegreen 2015). Based on *Myrmica* dissections and our current understanding of *Spiroplasma* biology, sMyr appears to be extracellular and present in the haemolymph (Ballinger et al. 2018; Herren et al. 2013), an apparent key difference with previously described cases of cladogenic symbiont acquisition in ants (Cabuslay et al. 2024; Degnan et al. 2004; Hu et al. 2023; Jackson et al. 2022). Infection of extracellular nutritional symbionts has been identified in tortoise and hispine beetles, dating back to ~60 million years ago (García-Lozano et al. 2024; González Porrás et al. 2024). These folivorous beetles evolved specialized organs at the foregut-midgut junction to house the nutritional symbionts (Fukumori et al. 2022; González Porrás et al. 2024). A potential extracellular haemolymph-residing lifestyle of sMyr raises questions on how vertical transmission is achieved and maintained. In termites, proctodeal trophallaxis (exchange of hindgut content between nest mates) allows for a stable vertical transmission route of gut bacteria over millions of years, resulting in a strong signal of co-speciation in contemporary lineages (Arora et al. 2023; Brune and Dietrich 2015). A firmicute symbiont commonly infects the hindgut of *Diacamma* ant workers but appears to be absent from the reproductive castes (gamergates and males). Here, social interactions are also implicated in the spread of the gut-associated symbiont (Shimoji et al. 2021). In *Myrmica*, trophallaxis and polygyny could contribute to the spread and vertical transmission of sMyr (Lenoir 1982). Alternatively, sMyr may solely follow an ovarian transmission route. In *Drosophila melanogaster*, sMel *Spiroplasma* enter the germ line by coopting the yolk uptake machinery, a transmission route that can lead to host specificity (Herren et al. 2013). Our observation of sMyr-infected eggs within an experimental *M. scabrinodis* colony currently favours ovarian transmission.

In contrast to herbivores that rely on nutritional symbionts, *Myrmica* ants do not feed on an imbalanced dietary supply of nutrients (Fiedler et al. 2007). Consistent with the predaceous lifestyle of *Myrmica*, our genomic analyses suggest that infection persistence is not mediated by nutrient provisioning by sMyr. Instead, we observe candidate *RIP* genes in sMyr genomes that might control protection against parasites (Ballinger and Perlman 2017, 2019). *Myrmica* colonies are commonly attacked by natural enemies, including mites, nematodes and fungi (Witek et al. 2014). However, *RIP* and *RIP*-like genes are highly diverse within *Spiroplasma*, and functional validation is required before reaching a conclusion of a potential role of sMyr in *Myrmica* resistance (Ballinger and Perlman 2019; Moore and Ballinger 2023). Alternatively, sMyr spread and persistence

in *Myrmica* could be associated with the induction of a reproductive phenotype, such as MK or CI. In three sMyr isolates, proteins with an OTU deubiquitinase domain were identified, a protein domain often coupled to MK and CI (Harumoto and Lemaitre 2018; Martinez et al. 2021). For Spaid toxins of sMel *Spiroplasma* that control MK, this deubiquitinase domain prevents degradation through the ubiquitin-proteasome pathway of the fly host (Harumoto 2023). Whereas MK *Spiroplasma* tend to segregate at low frequencies, defensive *Spiroplasma* can reach high infection frequencies in nature, as observed in some *Drosophila* populations (Cockburn et al. 2013; Montenegro et al. 2005; Watts et al. 2009). The near-fixation frequencies of sMyr would be more consistent with a defensive role. For the sMyr-infected *Myrmica* species group, ~96% of the workers tested positive, suggesting that sMyr is not an obligate symbiont for *Myrmica* workers.

sMyr *Spiroplasma* were not identified in our sampling of *M. rubra* and *M. ruginodis*, species that are placed outside the *scabrinodis* species group. In *M. ruginodis*, two variants, sRug1 and sRug2, were uncovered in queens and workers. However, one *M. ruginodis* queen and derived workers did not carry an infection, indicating that sRug1 and sRug2 are not obligate symbionts, at least under laboratory conditions. In workers of *M. ruginodis*, we observed a significantly lower infection frequency of sRug2 compared to sRug1. This could be caused by a preferential transmission of sRug2 towards queens. If sRug2 would mediate fitness penalties in workers, selection could further strengthen this transmission bias (Treanor et al. 2018). The different toxin repertoire of sRug1 versus sRug2 genomes could be interpreted as a signal of different transmission strategies. Alternatively, transmission rates to different castes could be equal but infection of sRug2 could be constrained in adult workers due to reduced development of reproductive tissues (Treanor et al. 2018). This would entail that sRug2 is concentrated in ovaries, whereas sRug1 would infect other tissues. Dissections of our *M. ruginodis* workers uncovered that various tissues, including head and mesosoma, carry a Citri infection. A pooled gaster sample was only infected with sRug1, suggesting that the spatial infection patterns may differ between these co-infecting variants. However, more dissection and genotyping efforts are required to derive a formal conclusion. Future studies should formally test a preferential versus constrained infection scenario for sRug1 and sRug2 by tracking infection frequencies through different tissues of queens, eggs, larvae and adult workers. Alternatively, sRug2 could manipulate caste differentiation in *M. ruginodis*, either indirectly by for instance altering larval feeding or directly by functioning as a caste-determining locus (Treanor et al. 2018).

By combining three DNA sequencing technologies, we uncovered intricate *Spiroplasma* co-infections in *Myrmica* that were not detected in previous work (Ballinger et al. 2018). A total of seven variants across the Citri and Ixodetis clade were identified, a likely underestimate of the total variant diversity in *Myrmica*. Additional variants may (co-)segregate in other *Myrmica* species, such as *M. schenki*. Our sampling of *Manica* colonies suggests that these cryptic co-infection patterns are restricted to the *Myrmica* genus. Our results are consistent with previous work that shows that insect taxa can carry independently acquired facultative symbionts with variable infection frequencies (Goryacheva et al. 2018; Haselkorn et al. 2009;

Moore and Ballinger 2023; Sanaei et al. 2021). Co-infection at the individual level may drive the spread of symbionts in host species through their combined effects on host reproduction (Engelstädter et al. 2004; Frank 1998; Miyata et al. 2024; Zug and Hammerstein 2018). *Wolbachia* of *M. scabrinodis* encode for an apparent functional Type I *cif* pair and may mediate CI in this insect host, facilitating the spread of co-infecting *sMyr*. Co-infections may also allow for recombination between *Spiroplasma* variants, resulting in an exchange of genes that underlie reproductive phenotypes, further driving the spread of symbionts in *Myrmica* hosts. Alternatively, co-infected hosts may have a greater fitness compared to the single infected ones, generating single infections by segregational loss. However, analyses of our current infection frequency data of *Myrmica* workers do not suggest reciprocal positive effects of co-infection on infection frequency.

To conclude, we reveal that *Spiroplasma* can display a complex continuum of infection heterogeneity that varies across castes in social insects and suggest that *Spiroplasma* can exhibit a cladogenic spread within insect hosts.

Author Contributions

N.W. conceived and designed the study. T.P., T.V.W., W.D. and N.W. performed field sampling. D.C.F., T.P., T.V.W., E.V.R. and N.W. performed molecular lab work. D.C.F., J.R. and N.W. analysed the short-read and long-read data. T.P. ran data statistics. N.W. wrote the manuscript and prepared the figures, with input from D.C.F. and T.P. All authors read and approved the manuscript.

Acknowledgements

We are indebted to Andy Vierstraete for his assistance during our ONT sequencing efforts. We thank Helena and Tadek Wybouw for their assistance during *Myrmica* collection in the dunes. We further thank the many students that contributed to this study during their training.

Funding

This work was supported by the European Union (ERC, HYBRIPEST, 101078288 to N.W.) and the Special Research Fund of Ghent University (202302/011 to N.W.). This work was further supported by the FWO Research Network EVENET.

Conflicts of Interest

The authors declare no conflicts of interest.

Data Availability Statement

Read and sequence data of the current study are stored within the PRJEB91907 project at the European Nucleotide Archive (ENA). The ONT read data of the 20 *Myrmica* queens can be accessed using ERR15284710 to ERR15284729. The *COI* sequences of *Myrmica* workers can be accessed using ERZ27266337. The Illumina read data of the 10 monogynous *Myrmica* colonies can be accessed using ERR16001960 to ERR16001969.

References

Akhter, S., R. K. Aziz, and R. A. Edwards. 2012. "PhiSpy: A Novel Algorithm for Finding Prophages in Bacterial Genomes That Combines Similarity- and Composition-Based Strategies." *Nucleic Acids Research* 40, no. 16: e126. <https://doi.org/10.1093/nar/gks406>.

Alneberg, J., B. S. Bjarnason, I. De Bruijn, et al. 2014. "Binning Metagenomic Contigs by Coverage and Composition." *Nature Methods* 11, no. 11: 1144–1146. <https://doi.org/10.1038/nmeth.3103>.

Amoros, J., M. Buysse, A. M. Floriano, et al. 2025. "Diversity and Spread of Cytoplasmic Incompatibility Genes Among Maternally Inherited Symbionts." *PLoS Genetics* 21, no. 9: e1011856. <https://doi.org/10.1371/journal.pgen.1011856>.

Arora, J., A. Buček, S. Hellemans, et al. 2023. "Evidence of Cospeciation Between Termites and Their Gut Bacteria on a Geological Time Scale." *Proceedings of the Royal Society B: Biological Sciences* 290: 20230619. <https://doi.org/10.1098/rspb.2023.0619>.

Ballinger, M. J., L. D. Moore, and S. J. Perlman. 2018. "Evolution and Diversity of Inherited *Spiroplasma* Symbionts in *Myrmica* Ants." *Applied and Environmental Microbiology* 84, no. 4: e02299-17. <https://doi.org/10.1128/AEM.02299-17>.

Ballinger, M. J., and S. J. Perlman. 2017. "Generality of Toxins in Defensive Symbiosis: Ribosome-Inactivating Proteins and Defense Against Parasitic Wasps in *Drosophila*." *PLoS Pathogens* 13, no. 7: e1006431. <https://doi.org/10.1371/journal.ppat.1006431>.

Ballinger, M. J., and S. J. Perlman. 2019. "The Defensive *Spiroplasma*." *Current Opinion in Insect Science* 32: 36–41. <https://doi.org/10.1016/j.cois.2018.10.004>.

Beckmann, J. F., J. A. Ronau, and M. Hochstrasser. 2017. "A *Wolbachia* Deubiquitylating Enzyme Induces Cytoplasmic Incompatibility." *Nature Microbiology* 2, no. 5: 17007. <https://doi.org/10.1038/nmicrobiol.2017.7>.

Bové, J. M., J. Renaudin, C. Saillard, X. Foissac, and M. Garnier. 2003. "*Spiroplasma citri*, a Plant Pathogenic Mollicute: Relationships With Its Two Hosts, the Plant and the Leafhopper Vector." *Annual Review of Phytopathology* 41, no. 1: 483–500. <https://doi.org/10.1146/annurev.phyto.41.052102.104034>.

Brenninger, F. A., R. Zug, and H. Kokko. 2025. "Infection Dynamics of Endosymbionts That Manipulate Arthropod Reproduction." *Biological Reviews* 100: brv.70024. <https://doi.org/10.1111/brv.70024>.

Brune, A., and C. Dietrich. 2015. "The Gut Microbiota of Termites: Digesting the Diversity in the Light of Ecology and Evolution." *Annual Review of Microbiology* 69, no. 1: 145–166. <https://doi.org/10.1146/annurev-micro-092412-155715>.

Cabuslay, C., J. T. Wertz, B. Béchade, et al. 2024. "Domestication and Evolutionary Histories of Specialized Gut Symbionts Across Cephalotine Ants." *Molecular Ecology* 33, no. 15: e17454. <https://doi.org/10.1111/mec.17454>.

Chaumeil, P.-A., A. J. Mussig, P. Hugenholtz, and D. H. Parks. 2022. "GTDB-Tk v2: Memory Friendly Classification With the Genome Taxonomy Database." *Bioinformatics* 38, no. 23: 5315–5316. <https://doi.org/10.1093/bioinformatics/btac672>.

Cheng, B., N. Kuppanda, J. C. Aldrich, O. S. Akbari, and P. M. Ferree. 2016. "Male-Killing *Spiroplasma* Alters Behavior of the Dosage Compensation Complex During *Drosophila melanogaster* Embryogenesis." *Current Biology* 26, no. 10: 1339–1345. <https://doi.org/10.1016/j.cub.2016.03.050>.

Chklovski, A., D. H. Parks, B. J. Woodcroft, and G. W. Tyson. 2023. "CheckM2: A Rapid, Scalable and Accurate Tool for Assessing Microbial Genome Quality Using Machine Learning." *Nature Methods* 20, no. 8: 1203–1212. <https://doi.org/10.1038/s41592-023-01940-w>.

Clark, T. B., R. F. Whitcomb, J. G. Tully, et al. 1985. "*Spiroplasma melliferum*, a New Species From the Honeybee (*Apis mellifera*)." *International Journal of Systematic Bacteriology* 35, no. 3: 296–308. <https://doi.org/10.1099/00207713-35-3-296>.

Cockburn, S. N., T. S. Haselkorn, P. T. Hamilton, E. Landzberg, J. Jaenike, and S. J. Perlman. 2013. "Dynamics of the Continent-Wide

- Spread of a *Drosophila* Defensive Symbiont." *Ecology Letters* 16, no. 5: 609–616. <https://doi.org/10.1111/ele.12087>.
- Couvin, D., A. Bernheim, C. Toffano-Nioche, et al. 2018. "CRISPRCasFinder, an Update of CRISPRFinder, Includes a Portable Version, Enhanced Performance and Integrates Search for Cas Proteins." *Nucleic Acids Research* 46, no. W1: W246–W251. <https://doi.org/10.1093/nar/gky425>.
- De Vienne, D. M., T. Giraud, and J. A. Shykoff. 2007. "When Can Host Shifts Produce Congruent Host and Parasite Phylogenies? A Simulation Approach." *Journal of Evolutionary Biology* 20, no. 4: 1428–1438. <https://doi.org/10.1111/j.1420-9101.2007.01340.x>.
- Degnan, P. H., A. B. Lazarus, C. D. Brock, and J. J. Wernegreen. 2004. "Host–Symbiont Stability and Fast Evolutionary Rates in an Ant–Bacterium Association: Cospeciation of *Camponotus* Species and Their Endosymbionts, Candidatus *Blochmannia*." *Systematic Biology* 53, no. 1: 95–110. <https://doi.org/10.1080/10635150490264842>.
- Ebsen, J. R., J. J. Boomsma, and D. R. Nash. 2019. "Phylogeography and Cryptic Speciation in the *Myrmica scabrinodis* NYLANDER, 1846 Species Complex (Hymenoptera: Formicidae), and Their Conservation Implications." *Insect Conservation and Diversity* 12, no. 6: 467–480. <https://doi.org/10.1111/icad.12366>.
- Eddy, S. R. 2011. "Accelerated Profile HMM Searches." *PLoS Computational Biology* 7, no. 10: e1002195. <https://doi.org/10.1371/journal.pcbi.1002195>.
- Edgar, R. C. 2010. "Search and Clustering Orders of Magnitude Faster Than BLAST." *Bioinformatics* 26, no. 19: 2460–2461. <https://doi.org/10.1093/bioinformatics/btq461>.
- Engelstädter, J., and G. D. D. Hurst. 2009. "The Ecology and Evolution of Microbes That Manipulate Host Reproduction." *Annual Review of Ecology, Evolution, and Systematics* 40, no. 1: 127–149. <https://doi.org/10.1146/annurev.ecolsys.110308.120206>.
- Engelstädter, J., A. Telschow, and P. Hammerstein. 2004. "Infection Dynamics of Different *Wolbachia*-Types Within One Host Population." *Journal of Theoretical Biology* 231, no. 3: 345–355. <https://doi.org/10.1016/j.jtbi.2004.06.029>.
- Eren, A. M., Ö. C. Esen, C. Quince, et al. 2015. "Anvi'o: An Advanced Analysis and Visualization Platform for Omics Data." *PeerJ* 3: e1319. <https://doi.org/10.7717/peerj.1319>.
- Evans, J. D. 1996. "Queen Longevity, Queen Adoption, and Posthumous Indirect Fitness in the Facultatively Polygynous Ant *Myrmica tahoensis*." *Behavioral Ecology and Sociobiology* 39, no. 4: 275–284. <https://doi.org/10.1007/s002650050290>.
- Fiedler, K., F. Kuhlmann, B. C. Schlick-Steiner, F. M. Steiner, and G. Gebauer. 2007. "Stable N-Isotope Signatures of Central European Ants – Assessing Positions in a Trophic Gradient." *Insectes Sociaux* 54, no. 4: 393–402. <https://doi.org/10.1007/s00040-007-0959-0>.
- Finn, R. D., J. Clements, and S. R. Eddy. 2011. "HMMER Web Server: Interactive Sequence Similarity Searching." *Nucleic Acids Research* 39, no. suppl: W29–W37. <https://doi.org/10.1093/nar/gkr367>.
- Frank, S. A. 1998. "Dynamics of Cytoplasmic Incompatibility With Multiple *Wolbachia* Infections." *Journal of Theoretical Biology* 192, no. 2: 213–218. <https://doi.org/10.1006/jtbi.1998.0652>.
- Fukumori, K., K. Oguchi, H. Ikeda, et al. 2022. "Evolutionary Dynamics of Host Organs for Microbial Symbiosis in Tortoise Leaf Beetles (Coleoptera: Chrysomelidae: Cassidinae)." *MBio* 13, no. 1: e03691-21. <https://doi.org/10.1128/mbio.03691-21>.
- García-Lozano, M., C. Henzler, M. Á. G. Porras, et al. 2024. "Paleocene Origin of a Streamlined Digestive Symbiosis in Leaf Beetles." *Current Biology* 34, no. 8: 1621–1634.e9. <https://doi.org/10.1016/j.cub.2024.01.070>.
- Gerth, M., H. Martínez-Montoya, P. Ramirez, et al. 2021. "Rapid Molecular Evolution of *Spiroplasma* Symbionts of *Drosophila*." *Microbial Genomics* 7, no. 2: 000503. <https://doi.org/10.1099/mgen.0.000503>.
- González Porras, M. Á., I. Pons, M. García-Lozano, et al. 2024. "Extracellular Symbiont Colonizes Insect During Embryo Development." *ISME Communications* 4, no. 1: ycae005. <https://doi.org/10.1093/ismeco/ycae005>.
- Goryacheva, I., A. Blekhman, B. Andrianov, D. Romanov, and I. Zakharov. 2018. "Spiroplasma Infection in *Harmonia axyridis*—Diversity and Multiple Infection." *PLoS One* 13, no. 5: e0198190. <https://doi.org/10.1371/journal.pone.0198190>.
- Gruber-Vodicka, H. R., B. K. B. Seah, and E. Pruesse. 2020. "phyloFlash: Rapid Small-Subunit rRNA Profiling and Targeted Assembly From Metagenomes." *mSystems* 5, no. 5: e00920-20. <https://doi.org/10.1128/mSystems.00920-20>.
- Hague, M. T. J., H. Mavengere, D. R. Matute, and B. S. Cooper. 2020. "Environmental and Genetic Contributions to Imperfect *w* Mel-Like *Wolbachia* Transmission and Frequency Variation." *Genetics* 215, no. 4: 1117–1132. <https://doi.org/10.1534/genetics.120.303330>.
- Hamm, C. A., D. J. Begun, A. Vo, et al. 2014. "*Wolbachia* Do Not Live by Reproductive Manipulation Alone: Infection Polymorphism in *Drosophila suzukii* and *D. subpulchrella*." *Molecular Ecology* 23, no. 19: 4871–4885. <https://doi.org/10.1111/mec.12901>.
- Harumoto, T. 2023. "Self-Stabilization Mechanism Encoded by a Bacterial Toxin Facilitates Reproductive Parasitism." *Current Biology* 33, no. 18: 4021–4029.e6. <https://doi.org/10.1016/j.cub.2023.08.032>.
- Harumoto, T., H. Anbutsu, B. Lemaitre, and T. Fukatsu. 2016. "Male-Killing Symbiont Damages Host's Dosage-Compensated Sex Chromosome to Induce Embryonic Apoptosis." *Nature Communications* 7, no. 1: 12781. <https://doi.org/10.1038/ncomm512781>.
- Harumoto, T., and B. Lemaitre. 2018. "Male-Killing Toxin in a Bacterial Symbiont of *Drosophila*." *Nature* 557, no. 7704: 252–255. <https://doi.org/10.1038/s41586-018-0086-2>.
- Haselkorn, T. S., T. A. Markow, and N. A. Moran. 2009. "Multiple Introductions of the *Spiroplasma* Bacterial Endosymbiont Into *Drosophila*." *Molecular Ecology* 18, no. 6: 1294–1305. <https://doi.org/10.1111/j.1365-294X.2009.04085.x>.
- He, L.-S., P.-W. Zhang, J.-M. Huang, F.-C. Zhu, A. Danchin, and Y. Wang. 2018. "The Enigmatic Genome of an Obligate Ancient *Spiroplasma* Symbiont in a Hadal Holothurian." *Applied and Environmental Microbiology* 84, no. 1: e01965-17. <https://doi.org/10.1128/AEM.01965-17>.
- Herren, J. K., J. C. Paredes, F. Schüpfer, and B. Lemaitre. 2013. "Vertical Transmission of a *Drosophila* Endosymbiont via Cooption of the Yolk Transport and Internalization Machinery." *MBio* 4, no. 2: e00532-12. <https://doi.org/10.1128/mBio.00532-12>.
- Hildebrand, A., M. Remmert, A. Biegert, and J. Söding. 2009. "Fast and Accurate Automatic Structure Prediction With HHpred." *Proteins: Structure, Function, and Bioinformatics* 77, no. S9: 128–132. <https://doi.org/10.1002/prot.22499>.
- Hoffmann, A. A., M. Turelli, and L. G. Harshman. 1990. "Factors Affecting the Distribution of Cytoplasmic Incompatibility in *Drosophila simulans*." *Genetics* 126, no. 4: 933–948. <https://doi.org/10.1093/genetics/126.4.933>.
- Hosokawa, T., Y. Kikuchi, N. Nikoh, M. Shimada, and T. Fukatsu. 2006. "Strict Host-Symbiont Cospeciation and Reductive Genome Evolution in Insect Gut Bacteria." *PLoS Biology* 4, no. 10: e337. <https://doi.org/10.1371/journal.pbio.0040337>.
- Hosokawa, T., N. Nikoh, R. Koga, et al. 2012. "Reductive Genome Evolution, Host–Symbiont Co-Speciation and Uterine Transmission of Endosymbiotic Bacteria in Bat Flies." *ISME Journal* 6, no. 3: 577–587. <https://doi.org/10.1038/ismej.2011.125>.

- Hu, Y., C. L. D'Amelio, B. Béchade, et al. 2023. "Partner Fidelity and Environmental Filtering Preserve Stage-Specific Turtle Ant Gut Symbioses for Over 40 Million Years." *Ecological Monographs* 93, no. 1: e1560. <https://doi.org/10.1002/ecm.1560>.
- Hurst, G. D. D., A. P. Johnson, J. H. Graf von der Schulenburg, and Y. Fuyama. 2000. "Male-Killing *Wolbachia* in *Drosophila*: A Temperature-Sensitive Trait With a Threshold Bacterial Density." *Genetics* 156, no. 2: 699–709.
- Itoh, H., S. Jang, K. Takeshita, et al. 2019. "Host–Symbiont Specificity Determined by Microbe–Microbe Competition in an Insect Gut." *Proceedings of the National Academy of Sciences* 116, no. 45: 22673–22682. <https://doi.org/10.1073/pnas.1912397116>.
- Jackson, R., D. Monnin, P. A. Patapiou, et al. 2022. "Convergent Evolution of a Labile Nutritional Symbiosis in Ants." *ISME Journal* 16, no. 9: 2114–2122. <https://doi.org/10.1038/s41396-022-01256-1>.
- Jones, P., D. Binns, H.-Y. Chang, et al. 2014. "InterProScan 5: Genome-Scale Protein Function Classification." *Bioinformatics* 30, no. 9: 1236–1240. <https://doi.org/10.1093/bioinformatics/btu031>.
- Kang, D. D., F. Li, E. Kirton, et al. 2019. "MetaBAT 2: An Adaptive Binning Algorithm for Robust and Efficient Genome Reconstruction From Metagenome Assemblies." *PeerJ* 7: e7359. <https://doi.org/10.7717/peerj.7359>.
- Katoh, K., and D. M. Standley. 2013. "MAFFT Multiple Sequence Alignment Software Version 7: Improvements in Performance and Usability." *Molecular Biology and Evolution* 30, no. 4: 772–780. <https://doi.org/10.1093/molbev/mst010>.
- Klein, A., L. Schrader, R. Gil, et al. 2016. "A Novel Intracellular Mutualistic Bacterium in the Invasive Ant *Cardiocondyla obscurior*." *ISME Journal* 10, no. 2: 376–388. <https://doi.org/10.1038/ismej.2015.119>.
- Kondo, N., M. Shimada, and T. Fukatsu. 2005. "Infection Density of *Wolbachia* Endosymbiont Affected by Co-Infection and Host Genotype." *Biology Letters* 1, no. 4: 488–491. <https://doi.org/10.1098/rsbl.2005.0340>.
- Langmead, B., and S. L. Salzberg. 2012. "Fast Gapped-Read Alignment With Bowtie 2." *Nature Methods* 9, no. 4: 357–359. <https://doi.org/10.1038/nmeth.1923>.
- Lenoir, A. 1982. "An Informational Analysis of Antennal Communication During Trophallaxis in the Ant *Myrmica rubra* L." *Behavioural Processes* 7, no. 1: 27–35. [https://doi.org/10.1016/0376-6357\(82\)90050-X](https://doi.org/10.1016/0376-6357(82)90050-X).
- LePage, D. P., J. A. Metcalf, S. R. Bordenstein, et al. 2017. "Prophage WO Genes Recapitulate and Enhance *Wolbachia*-Induced Cytoplasmic Incompatibility." *Nature* 543, no. 7644: 243–247. <https://doi.org/10.1038/nature21391>.
- Li, D., C.-M. Liu, R. Luo, K. Sadakane, and T.-W. Lam. 2015. "MEGAHIT: An Ultra-Fast Single-Node Solution for Large and Complex Metagenomics Assembly via Succinct de Bruijn Graph." *Bioinformatics* 31, no. 10: 1674–1676. <https://doi.org/10.1093/bioinformatics/btv033>.
- Liu, C.-C., S.-S. Dong, J.-B. Chen, et al. 2022. "MetaDecoder: A Novel Method for Clustering Metagenomic Contigs." *Microbiome* 10, no. 1: 46. <https://doi.org/10.1186/s40168-022-01237-8>.
- Martinez, J., L. Klasson, J. J. Welch, and F. M. Jiggins. 2021. "Life and Death of Selfish Genes: Comparative Genomics Reveals the Dynamic Evolution of Cytoplasmic Incompatibility." *Molecular Biology and Evolution* 38, no. 1: 2–15. <https://doi.org/10.1093/molbev/msaa209>.
- McCutcheon, J. P., B. M. Boyd, and C. Dale. 2019. "The Life of an Insect Endosymbiont From the Cradle to the Grave." *Current Biology* 29, no. 11: R485–R495. <https://doi.org/10.1016/j.cub.2019.03.032>.
- McCutcheon, J. P., and N. A. Moran. 2010. "Functional Convergence in Reduced Genomes of Bacterial Symbionts Spanning 200 My of Evolution." *Genome Biology and Evolution* 2: 708–718. <https://doi.org/10.1093/gbe/evq055>.
- Meng, G., Y. Li, C. Yang, and S. Liu. 2019. "MitoZ: A Toolkit for Animal Mitochondrial Genome Assembly, Annotation and Visualization." *Nucleic Acids Research* 47, no. 11: e63. <https://doi.org/10.1093/nar/gkz173>.
- Minh, B. Q., H. A. Schmidt, O. Chernomor, et al. 2020. "IQ-TREE 2: New Models and Efficient Methods for Phylogenetic Inference in the Genomic Era." *Molecular Biology and Evolution* 37, no. 5: 1530–1534. <https://doi.org/10.1093/molbev/msaa015>.
- Miyata, M., M. Nomura, and D. Kageyama. 2024. "Rapid Spread of a Vertically Transmitted Symbiont Induces Drastic Shifts in Butterfly Sex Ratio." *Current Biology: CB* 34, no. 10: R490–R492. <https://doi.org/10.1016/j.cub.2024.04.027>.
- Moar, W. J., A. J. Evans, C. R. Kessenich, et al. 2017. "The Sequence, Structural, and Functional Diversity Within a Protein Family and Implications for Specificity and Safety: The Case for ETX_MTX2 Insecticidal Proteins." *Journal of Invertebrate Pathology* 142: 50–59. <https://doi.org/10.1016/j.jip.2016.05.007>.
- Montenegro, H., V. N. Solferini, L. B. Klaczko, and G. D. D. Hurst. 2005. "Male-Killing *Spiroplasma* Naturally Infecting *Drosophila melanogaster*." *Insect Molecular Biology* 14, no. 3: 281–287. <https://doi.org/10.1111/j.1365-2583.2005.00558.x>.
- Moore, L. D., and M. J. Ballinger. 2023. "The Toxins of Vertically Transmitted *Spiroplasma*." *Frontiers in Microbiology* 14: 1148263. <https://doi.org/10.3389/fmicb.2023.1148263>.
- Morandini, C., M. M. Y. Tin, S. Abril, et al. 2016. "Comparative Transcriptomics Reveals the Conserved Building Blocks Involved in Parallel Evolution of Diverse Phenotypic Traits in Ants." *Genome Biology* 17, no. 1: 43. <https://doi.org/10.1186/s13059-016-0902-7>.
- Moreau, C. S., C. D. Bell, R. Vila, S. B. Archibald, and N. E. Pierce. 2006. "Phylogeny of the Ants: Diversification in the Age of Angiosperms." *Science* 312, no. 5770: 101–104. <https://doi.org/10.1126/science.1124891>.
- Nygaard, S., G. Zhang, M. Schiøtt, et al. 2011. "The Genome of the Leaf-Cutting Ant *Acromyrmex echinator* Suggests Key Adaptations to Advanced Social Life and Fungus Farming." *Genome Research* 21, no. 8: 1339–1348. <https://doi.org/10.1101/gr.121392.111>.
- Owashii, Y., H. Arai, T. Adachi-Hagimori, and D. Kageyama. 2024. "*Rickettsia* Induces Strong Cytoplasmic Incompatibility in a Predatory Insect." *Proceedings of the Royal Society B: Biological Sciences* 291, no. 2027: 20240680. <https://doi.org/10.1098/rspb.2024.0680>.
- Palma, L., D. Muñoz, C. Berry, J. Murillo, and P. Caballero. 2014. "*Bacillus thuringiensis* Toxins: An Overview of Their Biocidal Activity." *Toxins* 6, no. 12: 3296–3325. <https://doi.org/10.3390/toxins6123296>.
- Pedersen, J. S., and J. J. Boomsma. 1999. "Effect of Habitat Saturation on the Number and Turnover of Queens in the Polygynous Ant, *Myrmica sulcinodis*." *Journal of Evolutionary Biology* 12, no. 5: 903–917. <https://doi.org/10.1046/j.1420-9101.1999.00109.x>.
- Pollmann, M., L. D. Moore, E. Krimmer, et al. 2022. "Highly Transmissible Cytoplasmic Incompatibility by the Extracellular Insect Symbiont *Spiroplasma*." *iScience* 25, no. 5: 104335. <https://doi.org/10.1016/j.isci.2022.104335>.
- Quast, C., E. Pruesse, P. Yilmaz, et al. 2012. "The SILVA Ribosomal RNA Gene Database Project: Improved Data Processing and Web-Based Tools." *Nucleic Acids Research* 41, no. D1: D590–D596. <https://doi.org/10.1093/nar/gks1219>.
- Rambaut, A., A. J. Drummond, D. Xie, G. Baele, and M. A. Suchard. 2018. "Posterior Summarization in Bayesian Phylogenetics Using Tracer 1.7." *Systematic Biology* 67, no. 5: 901–904. <https://doi.org/10.1093/sysbio/syy032>.
- Rognes, T., T. Flouri, B. Nichols, C. Quince, and F. Mahé. 2016. "VSEARCH: A Versatile Open Source Tool for Metagenomics." *PeerJ* 4: e2584. <https://doi.org/10.7717/peerj.2584>.

- Romiguier, J., M. L. Borowiec, A. Weyna, et al. 2022. "Ant Phylogenomics Reveals a Natural Selection Hotspot Preceding the Origin of Complex Eusociality." *Current Biology* 32, no. 13: 2942–2947.e4. <https://doi.org/10.1016/j.cub.2022.05.001>.
- Ronquist, F., and J. P. Huelsenbeck. 2003. "MrBayes 3: Bayesian Phylogenetic Inference Under Mixed Models." *Bioinformatics* 19, no. 12: 1572–1574. <https://doi.org/10.1093/bioinformatics/btg180>.
- Saillard, C., J. C. Vignault, J. M. Bove, et al. 1987. "*Spiroplasma phoeniceum* Sp. Nov., a New Plant-Pathogenic Species From Syria." *International Journal of Systematic Bacteriology* 37, no. 2: 106–115. <https://doi.org/10.1099/00207713-37-2-106>.
- Sanaei, E., S. Charlat, and J. Engelstädter. 2021. "Wolbachia Host Shifts: Routes, Mechanisms, Constraints and Evolutionary Consequences." *Biological Reviews* 96, no. 2: 433–453. <https://doi.org/10.1111/brv.12663>.
- Schröder, D., H. Deppisch, M. Obermayer, et al. 1996. "Intracellular Endosymbiotic Bacteria of *Camponotus* Species (Carpenter Ants): Systematics, Evolution and Ultrastructural Characterization." *Molecular Microbiology* 21, no. 3: 479–489. <https://doi.org/10.1111/j.1365-2958.1996.tb02557.x>.
- Seemann, T. 2014. "Prokka: Rapid Prokaryotic Genome Annotation." *Bioinformatics* 30, no. 14: 2068–2069. <https://doi.org/10.1093/bioinformatics/btu153>.
- Seifert, B. 2007. *Die Ameisen Mittel- Und Nordeuropas*. Lutra Verlags- und Vertriebsgesellschaft.
- Seppy, M., M. Manni, and E. M. Zdobnov. 2019. "BUSCO: Assessing Genome Assembly and Annotation Completeness." In *Gene Prediction*, edited by M. Kollmar, vol. 1962, 227–245. Springer New York. https://doi.org/10.1007/978-1-4939-9173-0_14.
- Shimoji, H., H. Itoh, Y. Matsuura, et al. 2021. "Worker-Dependent Gut Symbiosis in an Ant." *ISME Communications* 1, no. 1: 60. <https://doi.org/10.1038/s43705-021-00061-9>.
- Shropshire, J. D., B. Leigh, and S. R. Bordenstein. 2020. "Symbiont-Mediated Cytoplasmic Incompatibility: What Have We Learned in 50 Years?" *eLife* 9: e61989. <https://doi.org/10.7554/eLife.61989>.
- Sieber, C. M. K., A. J. Probst, A. Sharrar, et al. 2018. "Recovery of Genomes From Metagenomes via a Dereplication, Aggregation and Scoring Strategy." *Nature Microbiology* 3, no. 7: 836–843. <https://doi.org/10.1038/s41564-018-0171-1>.
- Smith, C. R., C. D. Smith, H. M. Robertson, et al. 2011. "Draft Genome of the Red Harvester Ant *Pogonomyrmex barbatus*." *Proceedings of the National Academy of Sciences* 108, no. 14: 5667–5672. <https://doi.org/10.1073/pnas.1007901108>.
- Stamatakis, A. 2014. "RAxML Version 8: A Tool for Phylogenetic Analysis and Post-Analysis of Large Phylogenies." *Bioinformatics* 30, no. 9: 1312–1313. <https://doi.org/10.1093/bioinformatics/btu033>.
- Starikova, E. V., P. O. Tikhonova, N. A. Prianichnikov, et al. 2020. "Phigaro: High-Throughput Prophage Sequence Annotation." *Bioinformatics* 36, no. 12: 3882–3884. <https://doi.org/10.1093/bioinformatics/btaa250>.
- Tamas, L., L. Klasson, B. Canbäck, et al. 2002. "50 Million Years of Genomic Stasis in Endosymbiotic Bacteria." *Science* 296, no. 5577: 2376–2379. <https://doi.org/10.1126/science.1071278>.
- Treanor, D., T. Pamminger, and W. O. H. Hughes. 2018. "The Evolution of Caste-Biasing Symbionts in the Social Hymenoptera." *Insectes Sociaux* 65, no. 4: 513–519. <https://doi.org/10.1007/s00040-018-0638-3>.
- Vierstraete, A. R., and B. P. Braeckman. 2022. "Amplicon_sorter: A Tool for Reference-Free Amplicon Sorting Based on Sequence Similarity and for Building Consensus Sequences." *Ecology and Evolution* 12, no. 3: e8603. <https://doi.org/10.1002/ece3.8603>.
- Watts, T., T. S. Haselkorn, N. A. Moran, and T. A. Markow. 2009. "Variable Incidence of *Spiroplasma* Infections in Natural Populations of *Drosophila* Species." *PLoS One* 4, no. 5: e5703. <https://doi.org/10.1371/journal.pone.0005703>.
- Williams, L. E., and J. J. Wernegreen. 2015. "Genome Evolution in an Ancient Bacteria-Ant Symbiosis: Parallel Gene Loss Among *Blochmannia* Spanning the Origin of the Ant Tribe Camponotini." *PeerJ* 3: e881. <https://doi.org/10.7717/peerj.881>.
- Wishart, D. S., S. Han, S. Saha, et al. 2023. "PHASTEST: Faster Than PHASTER, Better Than PHAST." *Nucleic Acids Research* 51, no. W1: W443–W450. <https://doi.org/10.1093/nar/gkad382>.
- Witek, M., F. Barbero, and B. Markó. 2014. "Myrmica Ants Host Highly Diverse Parasitic Communities: From Social Parasites to Microbes." *Insectes Sociaux* 61, no. 4: 307–323. <https://doi.org/10.1007/s00040-014-0362-6>.
- Worsley, S. F., T. M. Innocent, N. A. Holmes, et al. 2021. "Competition-Based Screening Helps to Secure the Evolutionary Stability of a Defensive Microbiome." *BMC Biology* 19, no. 1: 205. <https://doi.org/10.1186/s12915-021-01142-w>.
- Wu, Y.-W., B. A. Simmons, and S. W. Singer. 2016. "MaxBin 2.0: An Automated Binning Algorithm to Recover Genomes From Multiple Metagenomic Datasets." *Bioinformatics* 32, no. 4: 605–607. <https://doi.org/10.1093/bioinformatics/btv638>.
- Yang, Z. 2007. "PAML 4: Phylogenetic Analysis by Maximum Likelihood." *Molecular Biology and Evolution* 24, no. 8: 1586–1591. <https://doi.org/10.1093/molbev/msm088>.
- Zug, R., and P. Hammerstein. 2018. "Evolution of Reproductive Parasites With Direct Fitness Benefits." *Heredity* 120, no. 3: 266–281. <https://doi.org/10.1038/s41437-017-0022-5>.

Supporting Information

Additional supporting information can be found online in the Supporting Information section. **Figure S1:** Citri and Ixodetis *Spiroplasma* co-infection typifies *Myrmica* queens. For seven *Myrmica* species, each row represents a queen microbiome, characterized by 16S rRNA amplicon ONT sequencing. OTUs were identified using a 99% threshold of similarity. A total of four *Spiroplasma* OTUs (including Citri and Ixodetis) were identified and were often found co-infecting *Myrmica* queens. **Figure S2:** ANI heatmap for the *Myrmica*-associated and reference *Spiroplasma* variants. For our 14 *Myrmica*-associated *Spiroplasma* variants, My-ID is provided within brackets. The sMyr isolate from a previous study is indicated by scabri within brackets (Ballinger et al. 2018). **Figure S3:** End-point diagnostic PCR assay using *ftsZ* primers does not amplify the locus of Ixodetis *Spiroplasma*. The commonly used *ftsZ* primer pair is indicated by *ftsZ_F2* and *ftsZ_R2*. The custom designed *ftsZ* primer pair is indicated by *sIx0_F* and *sIx0_R*. sMyr are Citri *Spiroplasma* variants, whereas sScab2 and sSpec2 are Ixodetis *Spiroplasma* variants. Position numbering is based on the complete *ftsZ* coding sequence of sScab2 *Spiroplasma*. A black background with white font indicates polymorphic sites between the Ixodetis and Citri primers. **Figure S4:** Complex *Spiroplasma* co-infection patterns in *Myrmica* are confirmed by the taxon-annotated GC/coverage plots of our monogynous colonies. Metagenome profiles of the 10 experimental monogynous *Myrmica* colonies, labelled My-1 to My-10 (followed by species name). *Spiroplasma* contigs are colour coded, with *Myrmica* contigs depicted in light grey. My-7M. *ruginodis* did not appear to be infected with *Spiroplasma*. Five *Myrmica* colonies carried multiple *Spiroplasma* variants (My-8, My-5, My-9, My-4 and My-1) (Figure 2). **Figure S5:** Phylogeny of 16S rRNA sequences from metagenomes supports *Spiroplasma* co-infection in *Myrmica*. Phylogenetic trees showing the distance among 16S rRNA sequences recovered by (A) anviget-sequences-for-hmm-hits using the Ribosomal rRNA model and (B) by mapping reads and SPADES assembly included in PhyloFlash. Both maximum-likelihood trees were generated using IQ-Tree2. Ultrafast bootstrap values of 100 are not shown. **Figure S6:** mtDNA phylogeny is consistent with our morphological species classification. Maximum-likelihood phylogeny using *COI* fragments identified six *Myrmica*

species in our collection of workers (a subset of 27 colonies), supporting our morphological classification. Tree was generated with IQ-Tree2. All support values higher than 85 are shown. Accessions of reference *COI* sequences are underlined. **Figure S7:** *Wolbachia* infection frequency varies across *Myrmica* colonies and species. Mitochondrial phylogeny shows *Wolbachia* infection patterns across six *Myrmica* species and *Manica rubida*. Number of sampled workers and colonies are delineated, with colony number within brackets. **Figure S8:** Sanger trace data at the *ftsZ* locus differentiate *sRug1* and *sRug2* in *M. ruginodis*. Variant identity was formally assessed by detecting heterozygosity/homozygosity at 18 variable positions (Table S4). Here, trace data are plotted for three exemplar workers that differ in infection state (*sRug1* infected, co-infection and *sRug2* infected). Trace data are colour coded with orange and purple to indicate peaks corresponding to *sRug1* and *sRug2*, respectively. Black indicates non-variable positions at the *ftsZ* locus. **Figure S9:** Phylogenomic evidence for a seven-million-year infection of *sMyr Spiroplasma* in *Myrmica* ants. Panel A shows the congruent phylogeny of mitochondria and *sMyr* within four *Myrmica* species. *sMyr* phylogeny was rooted with *S. melliferum* (CP029202), whereas *Myrmica* phylogeny was rooted with a mitochondrion from *M. hunteri* (BK012650). No support values are depicted when all three maximum-likelihood approaches identified a support value of 100. Values from IQ-Tree2, Mr. Bayes and RaxML are shown without brackets, within round brackets and within squared brackets. This phylogenetic reconstruction does not include the *M. scabrinodis* sample from Ballinger et al. 2018. Panel B shows the time-calibrated nuclear phylogeny of the four *sMyr*-infected *Myrmica* species using *P. barbatus* and *A. echinatio*r as outgroups. Age of the MRCA of the *sMyr*-infected *Myrmica* species group is estimated based on the nuclear sequence data. **Figure S10:** Phylogenomic reconstruction identifies *sRug1* and *sMyr* as closely related Citri lineages. The maximum-likelihood phylogeny is midpoint-rooted and constructed using 31 single-copy orthologs. For each *Spiroplasma* isolate, the host is described within brackets. No support values are depicted when the maximum-likelihood analysis identified a support value of 100. These results are consistent with our ANI analyses (Figure S2) and 16S rRNA phylogenies (Figure S5). This panel of Citri representatives was further used to identify absent and enriched metabolic features of *sMyr*. **Figure S11:** *Spiroplasma* of *Myrmica* encode for OTU-containing and candidate RIP proteins. Panels A and B show a maximum-likelihood phylogeny of OTU-containing and candidate RIP proteins, respectively. OTU phylogeny was midpoint rooted and RIP phylogeny was rooted with *E. coli* Shiga toxin subunit A. Proteins of *sMyr* isolates are shown in green, whereas proteins of *sSpec2*, *sScab2*, *sSabu2* and *sRub* are shown in bold. My-ID is delineated within brackets. **Figure S12:** *Wolbachia* of the My-1 *M. scabrinodis* colony carry a Type I *cif* operon. A maximum-likelihood phylogeny of concatenated CifA and CifB protein sequences is depicted. The tree is midpoint rooted. Ultrafast bootstrap values were estimated from 10,000 replicates. No support values are depicted when the maximum-likelihood analysis identified a support value of 100. Phylogeny places the *cif* pair encoded by *Wolbachia* of My-1 within Type I (indicated with an arrow). This phylogeny uses the nomenclature of Martinez et al. 2021. Later studies have adopted other nomenclatures (e.g., Amoros et al. 2025). **Data S1:** mec70341-sup-0002-Tables.xlsx. **Data S2:** mec70341-sup-0003-Supinfo01.pdf.